Numerical study of a Langevin model for the growth of wetting layers

Raúl Toral
Departament de Física, Universitat de les Illes Balears, 07071 Palma de Mallorca, Spain
and Physics Department, Kansas State University, Manhattan, Kansas 66506

Amitabha Chakrabarti
Physics Department, Kansas State University, Manhattan, Kansas 66506
(Received 4 September 1990)

We present results of a numerical study of a Langevin equation describing the growth of wetting layers that occur when a binary mixture phase separates in the presence of a wall that attracts one of the two components of the mixture. We focus on the asymptotic behavior of the layer thickness with time and compare our results with recent theoretical predictions, showing good qualitative agreement. We also formulate and check a scaling hypothesis for the time evolution of the density-profile function.

I. INTRODUCTION

Many binary mixtures undergo the process of phase seperation when quenched from a high-temperature phase to a point within the coexistence curve of the mixture.[1] In this process, domains rich in either of the two components A and B appear and grow with time. If the mixture is in contact with a solid wall which favors component B of the mixture, then a layer of the phase rich in the B component will develop between the wall and the A-rich phase. This situation occurs, for instance, in the mixture of two liquids, one of which wets the wall and the other does not. If hydrodynamic effects such as flow and convection can be neglected, the main mechanism for the growth of the wetting layer is the diffusion of B molecules through the A-rich phase to the B phase in contact with the wall.

The late stages of this diffusion-limited growth process have been studied theoretically by Lipowsky and Huse[2] for the case of stable or metastable bulk solutions. They have developed a theory in which the growth of the wetting layer thickness is characterized by an asymptotic power-law behavior with time. The exponent of the power law is determined by the parameters of the interaction potential between the wall and the molecules of the mixture.

The situation is different in the regime of unstable bulk phase. In this case, the domain growth law of Lifshitz and Slyozov[3] should be appropriate. According to this theory, domains of the minority phase nucleate in the bulk and at late times grow as $t^{1/3}$. In the presence of a wall, which preferentially attracts one particular component, the growth of the wetting layer of this component is given essentially by the same mechanism of domain growth in the bulk. Thus, both the bulk domains and the layer thickness are expected to grow as $t^{1/3}$.

A microscopic model for the study of these growth processes has been introduced by Jiang and Ebner.[4] It consists of an Ising lattice-gas model with Kawasaki (conserved order parameter) dynamics in the presence of a long-range interaction potential between the particles and the wall: the interaction being of different sign for each of the two components of this mixture. Jiang and Ebner also carried out extensive numerical studies of this model and compared their results with the theoretical predictions of Lipowsky and Huse.

In this paper we study the growth of wetting layers starting from a field-theoreticl model. The main ingredient of this model is a conserved field variable that represents the difference of concentrations between the two components of the mixture. The equation of motion associated with the field variable is given by a Langevin equation as proposed by Cahn, Hillard, and Cook.[5] We study numerical simulations of this model for different quench locations and make a detailed comparison with the results of Ref. 2. We find a good agreement between the theory and the numerical simulation, in the sense that the thickness of the wetting layer evolves in time as a power law with an exponent consistent with that predicted by Lipowsky and Huse. We also formulate and test a new scaling prediction for the density profile along the direction perpendicular of the wetting layer.

In Sec. II we introduce the model and explain the numerical methods used for the simulation. Section III presents the main results of the simulation and makes a comparison with the predictions of Lipowsky and Huse. The main conclusions are summarized in Sec. IV.

II. MODEL AND NUMERICAL METHODS

In the Cahn-Hillard-Cook approach to the kinetics of phase separation, one considers the following Langevin-type equation governing the evolution with time (τ) of the field variable $\phi(\mathbf{r},\tau)$, representing the difference of the local concentration of the two components of the mixture:

$$\frac{\partial\phi}{\partial\tau}=M\nabla^2\frac{\delta H}{\delta\phi}+\eta\ , \tag{1}$$

where $H(\{\phi\})$ is the Hamiltonian of the system including

the interaction with an external potential $V(\mathbf{r})$. It is assumed to have the following form:

$$H(\{\phi\})=H_0(\{\phi\})+k_BT\int d\mathbf{r}\, V(\mathbf{r})\phi(\mathbf{r}) , \quad (2)$$

where $H_0(\{\phi\})$ is the standard Landau-Ginzburg Hamiltonian:

$$H_0(\{\phi\})=k_BT\int d\mathbf{r}\left[\frac{b}{2}\phi^2+\frac{u}{4}\phi^2+\frac{K}{2}|\nabla\phi|^2\right] . \quad (3)$$

Particular expressions for $V(\mathbf{r})$ will be discussed later. In Eq. (3), k_B is the Boltzmann constant, T is the temperature, M is the mobility and b, u, and K are parameters characterizing the Hamiltonian. $\eta(\mathbf{r},\tau)$ is a zero-mean Gaussian distributed stochastic random-field process which is completely determined by the following correlations:

$$\langle\eta(\mathbf{r},\tau)\eta(\mathbf{r}',\tau')\rangle=-2Mk_BT\nabla^2\delta(\mathbf{r}-\mathbf{r}')\delta(\tau-\tau') . \quad (4)$$

This relation ensures, via the fluctuation-dissipation theorem, that the stationary solution of Eq. (1) will be distributed according to the Boltzmann distribution at temperature T.

The resulting equation of motion after performing the functional derivative of the Hamiltonian is

$$\frac{\partial\phi}{\partial\tau}=Mk_BT\nabla^2(b\phi+u\phi^3-K\nabla^2\phi+V)+\eta . \quad (5)$$

This equation can be cast in a much simpler form by suitable rescaling. Let us introduce a new time variable $t=\tau/(Mk_BTK)$, a new field $\psi=\sqrt{K}\,\phi$, a rescaled potential $v(\mathbf{r})=V(\mathbf{r})/K$, and new parameters $\theta=b/K$, $\chi=u/k^2$, in terms of which the equation of motion (5) becomes

$$\frac{\partial\psi}{\partial t}=\nabla^2(\theta\psi+\chi\psi^3-\nabla^2\psi+v)+\xi , \quad (6)$$

where the new stochastic random field ξ is still Gaussian distributed of zero mean and satisfies the following correlations:

$$\langle\xi(\mathbf{r},t)\xi(\mathbf{r}',t')\rangle=-2\nabla^2\delta(\mathbf{r}-\mathbf{r}')\delta(t-t') . \quad (7)$$

A simple way of generating ξ in the numerical calculations is to write it as the divergence of a vector random process $\boldsymbol{\epsilon}$, i.e., $\xi=\nabla\cdot\boldsymbol{\epsilon}$, where the components $\epsilon^{(i)}$, $i=1,\ldots,d$ of the vector $\boldsymbol{\epsilon}$ are Gaussian distributed random processes of zero mean and correlations given by

$$\langle\epsilon^{(i)}(\mathbf{r},t)\epsilon^{(j)}(\mathbf{r}',t')\rangle=2\delta_{i,j}\delta(\mathbf{r}-\mathbf{r}')\delta(t-t') . \quad (8)$$

Our simulation has focused on two-dimensional systems. The numerical integration of Eq. (6) has been performed by using a simple Euler integration method. The time step required for convergence is found to be $\delta t=0.01$. Due to the stochastic nature of the equation, the results have been averaged for 10–20 runs depending on the quench location. The spatial derivatives are calculated by introducing a lattice grid and considering only the evolution of field values ψ_i at location i of the grid. The divergence and the Laplacian operators are then replaced by their lattice counterparts

$$\nabla\cdot\boldsymbol{\epsilon}\rightarrow\sum_{\mu=1}^{d}\epsilon^{(i\mu)}-d\epsilon^{(i)} \quad (9)$$

and

$$\nabla^2\psi\rightarrow\sum_{\mu=1}^{2d}\psi_{i_\mu}-2d\psi_i . \quad (10)$$

The index i_μ runs over the nearest neighbors of lattice site i and we have considered the mesh size to be equal to unity. Equation (1) ensures that the system order parameter $\langle\psi\rangle$ is a conserved quantity. Here, $\langle\psi\rangle$ is defined by

$$\langle\psi\rangle=N^{-1}\sum_{i=1}^{N}\psi_i , \quad (11)$$

the sum running over the N lattice sites.

In the numerical simulations, we have considered a rectangle of dimensions $[-L_2,L_2]\times[0,L_1]$. Typically, we have chosen $L_1=40$, $L_2=40$ but we have checked that the other values for L_1 and L_2 do not modify our results. The substrate is located at the line $X=0$. The potential $v(\mathbf{r})$ is considered to depend only on the distance x from the substrate line. In this way, the wetting layer develops on both sides of the line $x=0$. This construction allows us to use periodic boundary conditions in both x and y directions. The specific form considered for the interaction potential is

$$v(x)=\begin{cases}\dfrac{\sigma}{|x|^{p+1}}, & |x|\geq 0.5 ,\\ 2^{(p+1)}\sigma, & |x|\leq 0.5 .\end{cases} \quad (12)$$

Since the theoretical predictions for the growth-law exponent depend on the quench location, it is essential to determine the phase diagram of the model as accurately as possible. We have recently carried out[6] a calculation of the phase diagram for the "pure" system [when there is no interaction potential $v(\mathbf{r})$], by using a heat-bath

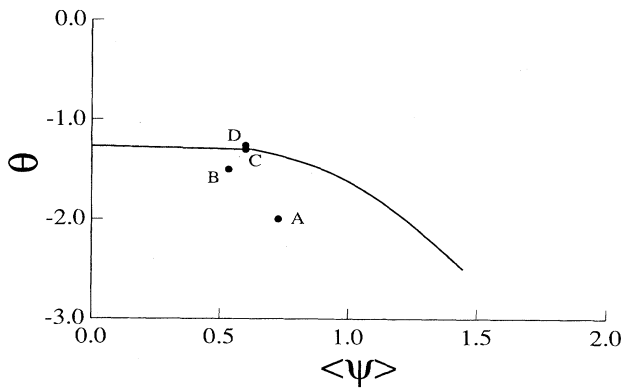

FIG. 1. Phase diagram of the ϕ^4 model defined by the Hamiltonian H_0 in Eq. (3) with $\chi=1$. The critical value is $\theta_c=-1.265$. The solid circles represent the location of the quenches studied in this work. The average order parameters for each of the quenches are as follows: $\langle\psi\rangle_A=0.7272$, $\langle\psi\rangle_B=0.543$, $\langle\psi\rangle_C=0.6$, and $\langle\psi\rangle_D-0.6$.

Monte Carlo method combined with extrapolation techniques.[7] Throughout the simulations we have considered the values $\chi=1$, $p=1$ and $\sigma=0.1$. Figure 1 shows the phase diagram for this particular value of χ. The critical value of θ is found to be $\theta_c=-1.265$. The values of $\langle\psi\rangle$ at coexistence for other θ values considered in the simulations are as follows:

$$\langle\psi\rangle^{(c)}_{(\theta=-1,3)}=0.630\ ,$$

$$\langle\psi\rangle^{(c)}_{(\theta=-1.5)}=0.8998\ ,$$

and

$$\langle\psi\rangle^{(c)}_{(\theta=-2)}=1.2204\ .$$

We report here the results coming from four particular quench locations, denoted by A, B, C, and D in Fig. 1. The particular values of the parameters used for those simulations are given in the caption of Fig. 1.

We have measured the time variation of the density profile function $n(r,t)$, along the x direction. This is defined as

$$n(r,t)=\frac{1}{2L_1}\sum_{i=1}^{L_1}[\psi(\mathbf{r}=(x,i),t)+\psi(\mathbf{r}=(-x,i),t)]\ . \tag{13}$$

The thickness of the wetting layer is obtained from the density profile as the value $l(t)$ that satisfies

$$n(l(t),t)=0\ . \tag{14}$$

III. RESULTS

Figures 2 show the final stages of the configuration for quenches B and C. In these figures, the layer develops on both sides of the substrate line $x=0$, located at the center of the figures. For quench B we note that the layer thickness is much larger than the corresponding one for quench C at the same time ($t=5000$).

Depending on the final location of the quench, we can distinguish two different behaviors: if the quench location is near the coexistence curve, Lipowsky and Huse predict that the intermediate time regime is described by a growth of the layer thickness according to a power law: $l(t)\propto t^n$. The exponent n is related to the exponent p [see Eq. (12)] as $n=1/(2(p+1))$. For the same quench location, the final approach to equilibrium is predicted to behave as[2,8]

$$l(t)-l(\infty)\propto t^{-1/2}\ ,$$

$l(\infty)$ being the equilibrium layer thickness.

As mentioned earlier, a different behavior is obtained if the quench location is such that the system is left in a point in the phase diagram deep inside the coexistence curve. In that case, the theory of Lifshitz and Slyozov predicts that the layer thickness should grow as $l(t)\propto t^{1/3}$.

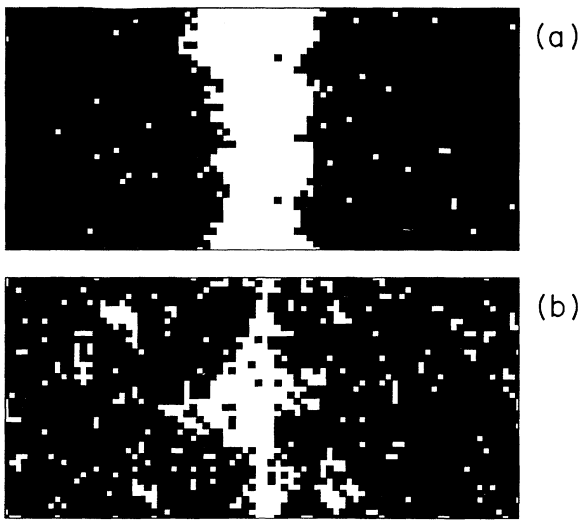

FIG. 2 (a) A typical configuration showing the presence of a layer rich in one of the two components, for quench at location B (see Fig. 1) after a time $t=5000$. The layer develops on both sides of the substrate line $x=0$, located at the center of the figure. (b) Same as (a) for quench C.

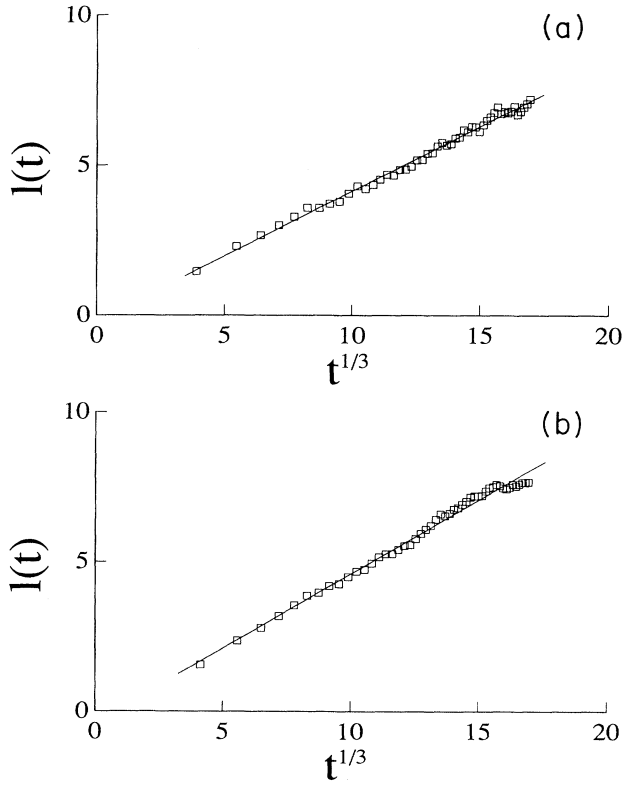

FIG. 3 (a) The layer thickness $l(t)$ plotted vs $t^{1/3}$ in case A corresponding to the growth of layers from an unstable bulk solution. The solid line is the least-squares fit to the data. We can see that the Lifshitz-Slyozov prediction $l(t)\propto t^{1/3}$ is well verified in this case. (b) Same as (a) for case B which corresponds again to the growth of layers starting from an unstable bulk solution but closer to coexistence than case A. The solid line is the least-squares fit to the data. The Lifshitz-Slyozov prediction $l(t)\propto t^{1/3}$ is well verified in this case.

Of the four quenches locations depicted in Fig. 1, quenches A and B are well inside the coexistence region. We plot, in Figs. 3(a) and 3(b), the layer thickness $l(t)$ versus $t^{1/3}$ to show that, in both cases, the Lifshitz-Slyozov law in well satisfied. We do not observe any difference between the two sets of data, even though quench B is closer to coexistence than quench A.

Quenches C and D (Fig. 1) are very close to the coexistence curve. Quench C is actually on the coexistence curve and quench D is just above coexistence. According to the theoretical results, we distinguish between intermediate times (growth of layers) and late times (approach to equilibrium). Figures 4(a) and 4(b) show the layer thickness $l(t)$ plotted versus $t^{1/6}$ for quenches C and D, respectively. The exponent $\frac{1}{6}$ is the theoretical prediction corresponding to $p=1$ in the interaction potential [Eq. (12)]. These plots show that, effectively, a power-law behavior characterized by an exponent $n=\frac{1}{6}$ is consistent with the simulation data for early to intermediate times. We see in Figs. 4(a) and 4(b) that the power-law behavior breaks down after a time $t \approx 1200$ for both quenches C and D. In Figs. 5(a) and 5(b) the same data are plotted versus $t^{-1/2}$ to check the asymptotic approach to equilib-

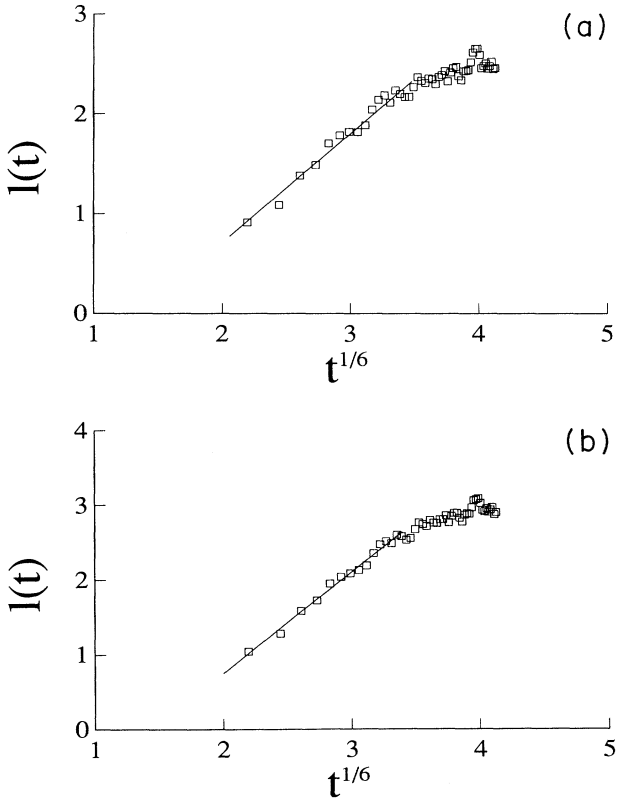

FIG. 4 (a) The layer thickness $l(t)$ plotted vs $t^{1/6}$ for case D. The exponent 1/6 corresponds to the prediction of the Lipowsky and Huse theory for the growth of layers from a stable phase. This predicted behavior breaks down for $t \geq 1200$ where a different functional form is expected as shown in Figs. 5. (b) Same as (a) for case C.

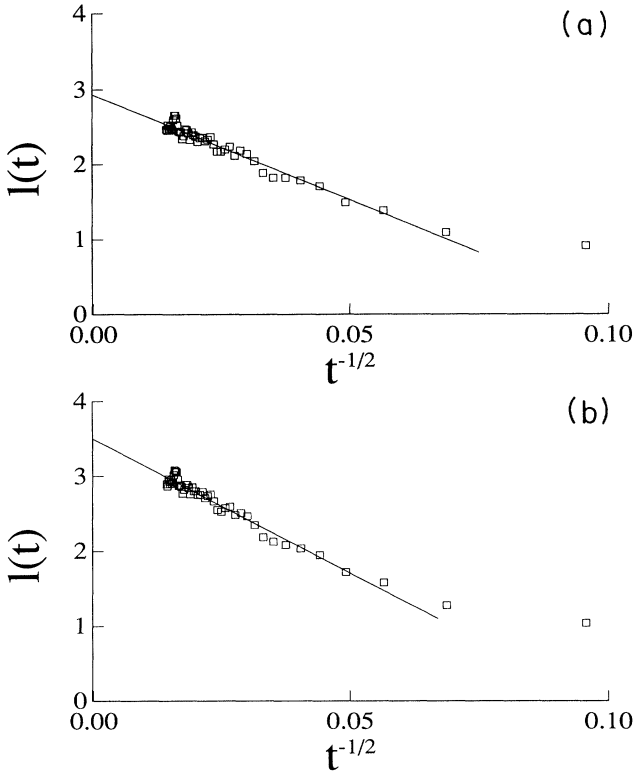

FIG. 5 (a) Plot of the layer thickness $l(t)$ vs $T^{-1/2}$ to check the prediction $l(t)-l(\infty) \propto t^{-1/2}$ in case D. (b) Same as (a) for case C.

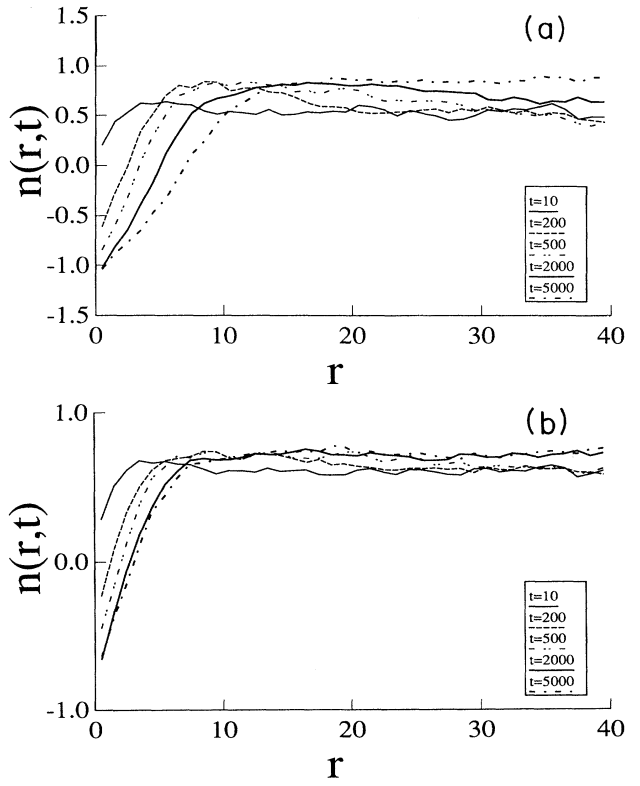

FIG. 6 (a) Density profile function $n(r,t)$ vs r for quench location B at different times. (b) Same as (a) for case C.

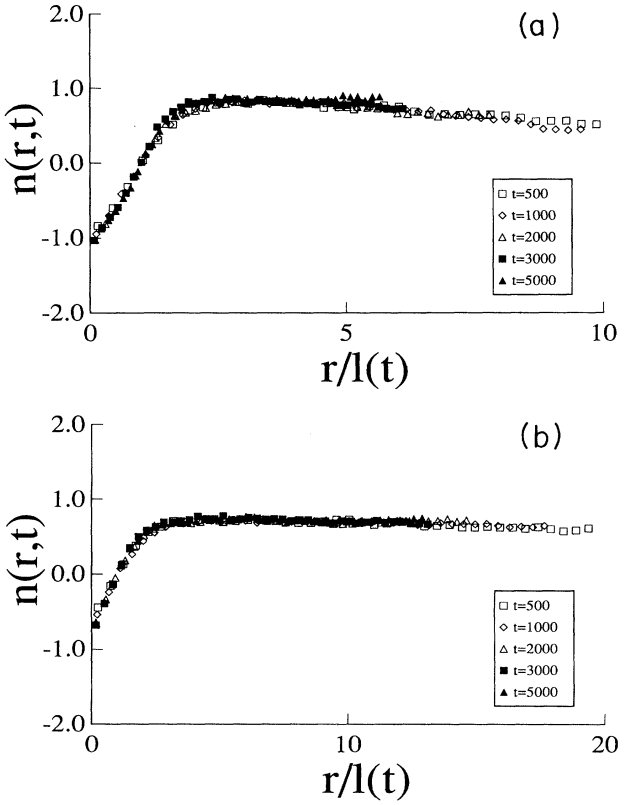

FIG. 7 (a) Test of the scaling hypothesis [Eq. (15)] for quench B, by plotting $n(r,t)$ vs the rescaled variable $r/l(t)$. Scaling holds quite well for $t \geq 500$. (b) Same as (a) for case C. Again the scaling hypothesis [Eq. (15)], is well satisfied for $t \geq 500$.

rium predicted by the theory. The data are fully consistent with the theoretical prediction in both cases.

We now present results for the evolution of the density profile function $n(r,t)$. In Figs. 6(a) and 6(b) we plot $n(r,t)$ versus r for different times after the quench. One expects that, at the late stages of evolution, the layer thickness is the only length scale in the problem. We then propose a dynamical scaling hypothesis[1] for the density profile function in the following way:

$$n(r,t)=n(r/l(t)) \ . \tag{15}$$

Figures 7(a) and 7(b) show the density profile function plotted versus $r/l(t)$ for quenches B and C, respectively (similar graphs are obtained in other quench locations). We can see from these figures that scaling is well satisfied at late enough times.

IV. CONCLUSIONS

We have studied numerically a Langevin equation describing the growth of wetting layers following a quench of a binary mixture in contact with a wall that favors one of the two components. We have studied the dependence of the layer thickness and the density profile function on the quench location. For quenches deep inside the coexistence curve, we have found that the layer thickness has a power-law growth with an exponent of $\frac{1}{3}$ as predicted by the Lifshitz-Slyozov theory. For quenches near coexistence, two different regimes have been considered: intermediate and late times. For intermediate times, the layer thickness grows as $t^{1/6}$, whereas the approach to equilibrium is described by the law[2,8]

$$l(t)-1(\infty) \propto t^{-1/2} \ .$$

These two behaviors are consistent with the theoretical predictions of Lipowsky and Huse. We want to stress, however, that it is very difficult to make a detailed quantitative comparison of the full predictions of the theory (such as the prefactors of the asymptotic power-law behavior). Also, due to the smallness of the predicted exponent ($\frac{1}{6}$) for intermediate times it is difficult to exclude other behaviors (such as other small exponents or even a logarithmic growth).

We have also introduced a dynamical scaling hypothesis for the density profile function for late enough times. This scaling should be valid when the layer thickness is the only length scale in the problem. We demonstrate by numerical simulations that the scaling hypothesis is actually very well satisfied at late times for the quenches considered in this study.

ACKNOWLEDGMENTS

R.T. acknowledges financial support from Direccion General de Investigacion Cientifica y Technica Project No. PB-86-0534 (Spain). The computations were carried out using the Cornell National Supercomputer Facility, a resource of the Cornell Theory Center, which is funded in part by the National Science Foundation, New York State, the IBM Corporation and the members of the Center's Corporate Research Institute. We thank Doug Durian and Andrea Liu for useful discussions.

[1]For a review, see J. Gunton, M. San Miguel, and P. Sahni, in *Phase Transitions and Critical Phenomena,* edited by C. Domb and J. Lebowitz (Academic, London, 1983), Vol. 8.
[2]R. Lipowsky and D. Huse, Phys. Rev. Lett. **57**, 353 (1986).
[3]I. Lifshitz and V. Slyozov, J. Phys. Chem. Solids **19**, 53 (1961).
[4]Z. Jiang and C. Ebner, Phys. Rev. B **39**, 2501 (1989).
[5]J. Cahn and J. Hilliard, J. Chem. Phys. **28**, 258 (1958); H. Cook, Acta Metall. **18**, 297 (1970).
[6]R. Toral and A. Chakrabarti, Phys. Rev. B **42**, 2445 (1990).
[7]A. Ferrenberg and R. Swendsen, Phys. Rev. Lett. **61**, 2635 (1988); **63**, 1195 (1989).
[8]For an experimental study and further theoretical discussions, see D. J. Durian and C. Franck, Phys. Rev. A **40**, 5220 (1989) and D. J. Durian, Ph.D. Thesis, Cornell University, 1989 (unpublished).